Published in final edited form as:
Gastroenterology. 2018 March 01; 154(4): 1080–1095. doi:10.1053/j.gastro.2017.11.002.

Mouse Model of Alagille Syndrome and Mechanisms of Jagged1 Missense Mutations

Emma R. Andersson[1,2,*], **Indira V. Chivukula**[1,11,*], **Simona Hankeova**[1,2,3,*], **Marika Sjöqvist**[2], **Yat Long Tsoi**[1], **Daniel Ramsköld**[4], **Jan Masek**[2], **Aiman Elmansuri**[2], **Anita Hoogendoorn**[2], **Elenae Vazquez**[5], **Helena Storvall**[9], **Julie Netušilová**[3], **Meritxell Huch**[6,7], **Björn Fischler**[8], **Ewa Ellis**[9], **Adriana Contreras**[5], **Antal Nemeth**[8], **Kenneth C. Chien**[1], **Hans Clevers**[6], **Rickard Sandberg**[10], **Vitezslav Bryja**[3], **Urban Lendahl**[1]

[1]Department of Cell and Molecular Biology, Karolinska Institutet, Stockholm, Sweden
[2]Department of Biosciences and Nutrition, Karolinska Institutet, Stockholm, Sweden [3]Institute of Experimental Biology, Faculty of Science, Masaryk University, Brno, Czech Republic
[4]Rheumatology Unit, Department of Medicine Solna, Karolinska Institutet, Karolinska University Hospital, Stockholm, Sweden [5]Unidad de Investigación Biomédica en Cáncer, Instituto Nacional de Cancerología-Instituto de Investigaciones Biomédicas, Universidad Nacional Autónoma de México, México City, México [6]Hubrecht Institute for Developmental Biology and Stem Cell Research, University Medical Centre Utrecht, Netherlands [8]Karolinska University Hospital, Department of Pediatrics, CLINTEC, Karolinska Institutet, Stockholm, Sweden [9]Karolinska University Hospital, CLINTEC, Karolinska Institutet, Stockholm, Sweden [10]Ludwig Institute for Cancer Research, Karolinska Institutet, Stockholm, Sweden

Abstract

Address requests for reprints to: Urban Lendahl, PhD, Karolinska Institutet, CMB, von Eulers väg 3, 17177 Stockholm, Sweden. urban.lendahl@ki.se. or, Emma R. Andersson, PhD, Karolinska Institutet, BioNut, Novum, 14183 Huddinge, Sweden. emma.andersson@ki.se.
[7]Present address: The Wellcome Trust/CRUK Gurdon Institute, Tennis Court Road, CB2, 1QN, Cambridge, UK
[11]Current affiliation: Integrated Cardio Metabolic Centre (ICMC), Karolinska Institutet, Huddinge, Sweden
[*]Authors share co-first authorship.

Author contributions: E.R.A., U.L.: Author study concept and design; acquisition of data; analysis and interpretation of data; drafting of the manuscript; critical revision of the manuscript for important intellectual content; statistical analysis; obtained funding; administrative, technical, or material support; study supervision. V.B.: Critical revision of the manuscript for important intellectual content; obtained funding; technical or material support; study supervision. I.V.C., S.H.: Acquisition of data; analysis and interpretation of data; drafting of the manuscript; critical revision of the manuscript for important intellectual content; statistical analysis. D.R., Y.L.T., R.S., E.V., H.S.: Analysis and interpretation of data; statistical analysis. M.S.: Acquisition of data; analysis and interpretation of data; statistical analysis; study supervision. J.N., A.E.: Acquisition of data; analysis and interpretation of data. A.H., J.M.: Acquisition of data; analysis and interpretation of data; statistical analysis. M.H.: Technical and material support; critical revision of the manuscript for important intellectual content. B.F., E.E., A.N., K.C., H.C., A.P.: Critical revision of the manuscript for important intellectual content; intellectual development of project, and material support (samples and/or methods).
Deposited data: GSE104876 is the reference series for this manuscript (https://www.ncbi.nlm.nih.gov/geo/query/acc.cgi?acc=GSE104876). GSE104873: RNA seq of livers from patients with Alagille syndrome (Figures 4 and 5) (https://www.ncbi.nlm.nih.gov/geo/query/acc.cgi?acc=GSE104873). GSE104874: Species specific transcriptomic data (mouse) of mouse C2C12 cells cocultured with human JAG1- or JAG1^{Ndr}-expressing cells (Figure 5) (https://www.ncbi.nlm.nih.gov/geo/query/acc.cgi?acc=GSE104874). GSE104875: RNA Seq of Jag1$^{Ndr/Ndr}$ and Jag1$^{+/+}$ liver (Figure 6) (https://www.ncbi.nlm.nih.gov/geo/query/acc.cgi?acc=GSE104875).

Conflicts of interest
The authors disclose no conflicts. A separate project in ERA lab is funded by ModeRNA.

Europe PMC Funders Author Manuscripts

Background & Aims—Alagille syndrome is a genetic disorder characterized by cholestasis, ocular abnormalities, characteristic facial features, heart defects, and vertebral malformations. Most cases are associated with mutations in *JAGGED1* (*JAG1*), which encodes a Notch ligand, although it is not clear how these contribute to disease development. We aimed to develop a mouse model of Alagille syndrome to elucidate these mechanisms.

Methods—Mice with a missense mutation (H268Q) in *Jag1* (*Jag1*$^{+/Ndr}$ mice) were outbred to a C3H/C57bl6 background to generate a mouse model for Alagille syndrome (*Jag1*$^{Ndr/Ndr}$ mice). Liver tissues were collected at different timepoints during development, analyzed by histology, and liver organoids were cultured and analyzed. We performed transcriptome analysis of *Jag1*$^{Ndr/Ndr}$ livers and livers from patients with Alagille syndrome, cross-referenced to the Human Protein Atlas, to identify commonly dysregulated pathways and biliary markers. We used species-specific transcriptome separation and ligand-receptor interaction assays to measure Notch signaling and the ability of JAG1^{Ndr} to bind or activate Notch receptors. We studied signaling of JAG1 and JAG1^{Ndr} via NOTCH 1, NOTCH2, and NOTCH3 and resulting gene expression patterns in parental and NOTCH1-expressing C2C12 cell lines.

Results—*Jag1*$^{Ndr/Ndr}$ mice had many features of Alagille syndrome, including eye, heart, and liver defects. Bile duct differentiation, morphogenesis, and function were dysregulated in newborn *Jag1*$^{Ndr/Ndr}$ mice, with aberrations in cholangiocyte polarity, but these defects improved in adult mice. *Jag1*$^{Ndr/Ndr}$ liver organoids collapsed in culture, indicating structural instability. Whole-transcriptome sequence analyses of liver tissues from mice and patients with Alagille syndrome identified dysregulated genes encoding proteins enriched at the apical side of cholangiocytes, including *CFTR* and *SLC5A1*, as well as reduced expression of *IGF1*. Exposure of Notch-expressing cells to JAG1^{Ndr}, compared with JAG1, led to hypomorphic Notch signaling, based on transcriptome analysis. JAG1-expressing cells, but not JAG1^{Ndr}-expressing cells, bound soluble Notch1 extracellular domain, quantified by flow cytometry. However, JAG1 and JAG1^{Ndr} cells each bound NOTCH2, and signaling from NOTCH2 signaling was reduced but not completely inhibited, in response to JAG1^{Ndr} compared with JAG1.

Conclusions—In mice, expression of a missense mutant of *Jag1* (*Jag1*^{Ndr}) disrupts bile duct development and recapitulates Alagille syndrome phenotypes in heart, eye, and craniofacial dysmorphology. JAG1^{Ndr} does not bind NOTCH1, but binds NOTCH2, and elicits hypomorphic signaling. This mouse model can be used to study other features of Alagille syndrome and organ development.

Keywords

Notch; Jagged1; Alagille; Heart; Liver; Kidney; Vertebrae; Development

Notch signaling is a highly conserved cell-contact–dependent signaling pathway used reiteratively in many developmental processes. Mutations in the Notch pathway lead to numerous diseases,[1] including Alagille syndrome (ALGS1; Online Mendelian Inheritance in Man/OMIM no. 118450, and ALGS2, OMIM no. 610205).[2] ALGS is an autosomal dominant genetic disorder that in more than 90% of patients is caused by mutations in *JAGGED1* (*JAG1*),[3,4] while about 1% harbor *NOTCH2* mutations.[5] Alagille syndrome often

presents early in life with severe liver and heart defects,[6] but also affects vertebrae, eyes, and craniofacial morphology.

How Alagille *JAG1* mutations affect signaling through different Notch receptors is poorly understood. The JAG1 ligand is expressed on a signal-sending cell that activates signaling upon contact with a Notch receptor on a juxta-posed signal-receiving cell. Missense mutations in ALGS are enriched in the receptor-binding DSL and DOS domains[1] of JAG1, and analysis of the crystallized JAG1 receptor-binding domain and an extracellular portion of NOTCH1[7] shows that the previously described *Jag1*^{Ndr} mutation[8] maps to this interaction domain, but how the *JAG1*^{Ndr} mutation mechanistically affects Notch signaling through receptors other than NOTCH1 remains to be established.

Deletions in a single *JAG1* allele are sufficient to cause ALGS, suggesting haploinsufficiency is the disease-causing mechanism. This is also supported by various mouse models, based on targeting *Jag1* and/or *Notch2* (for review, see [1]). Mouse models for ALGS liver disease include conditional *Jag1* ablation in portal vein mesenchyme,[9] and *Jag1/Notch2* compound heterozygous mice.[10,11] However, the first model does not mimic the full syndrome, and the *Jag1/Notch2* model biases our understanding of ALGS towards *Jag1/Notch2*-regulated conditions, though *NOTCH2* mutations are observed in only a fraction of ALGS cases.[12] Also, *NOTCH2*-related ALGS2 presents differently from *JAG1*-related ALGS1; for example, patients with *NOTCH2* mutations less frequently display heart defects.[13] *Jag1*$^{+/dDSL}$ mice on a C57bl6 background display bile duct paucity but are not jaundiced,[14] and it is unknown whether these mice recapitulate other major features of ALGS. Thus, the link between missense *Jag1* mutations and ALGS has not yet been possible to address in vivo.

In this report, we show that a missense mutation in *Jag1* (H268Q; Nodder, *Jag1*^{Ndr} [8]) generates a mouse model for ALGS, mimicking disease pathology in eye, craniofacial morphology, heart, and liver. By investigating liver development at different stages, and using liver organoids from *Jag1*$^{Ndr/Ndr}$ mice, we show that while biliary differentiation is delayed, biliary morphogenesis and maintenance are disrupted. In line with dysregulated morphogenesis, whole transcriptome analysis of ALGS liver biopsies and *Jag1*$^{Ndr/Ndr}$ livers confirms dysregulated expression of cell polarity genes, but not of key regulators of bile duct differentiation at postnatal or adult stages. At the molecular level, the JAG1^{Ndr} mutation generates a hypomorphic ligand that is unable to bind to specific Notch receptors: JAG1^{Ndr} binds NOTCH2, but not NOTCH1, and to a lesser degree NOTCH3. Collectively, we show that a missense mutation in *Jag1* is sufficient to invoke an ALGS phenotype in mice, and provide the first evidence that a *Jag1* missense mutation can impact differentially on different Notch receptor interactions.

Methods

Mouse Maintenance, Breeding, and Genetics

Jag1$^{+/Ndr}$ mice have been described previously,[8] and for the present study were maintained in a mixed C3H/C57bl6 genetic background. For details, see Supplementary Materials.

Measurement of Craniofacial Proportions

The distance from the eye to the snout tip and from the snout/forehead bridge to the snout tip were measured using ImageJ in images of E15.5 embryos taken from the animal's right side. All measurements were performed by experimenters blinded to the genotype.

Antibodies, Immunohistochemistry, and Staining

Fourteen-μm cryosections of liver were stained using routine staining protocols. For antibodies and staining details, see Supplementary Materials.

Bile Duct Quantification

Bile ducts in 10–100 portal triads were quantified per stage in *Jag1*$^{+/+}$ and *Jag1*$^{Ndr/Ndr}$ mice. For details, see Supplementary Materials.

Blood Chemistry Analysis

Plasma and serum were sent to the Swedish University of Agricultural Sciences for analysis of blood chemistry. For details, see Supplementary Materials.

Quantitative real-time polymerase chain reaction (qPCR)

qPCR was performed, as described.[15] For primers see Supplementary Materials.

Liver Organoid Cell Culture

Liver organoids were isolated and cultured, as described,[16] in the presence of R-spondin.

Collection of Human Samples for RNA Sequencing

Human liver needle biopsies were collected for clinical purposes, and a small part (3–5 mm x 1 mm) was snap-frozen and stored at -80°C. Diagnosis details are in Supplementary Materials.

Tissue Dissection, Homogenization, RNA Extraction, and cDNA Library Preparation

Liver was homogenized and RNA from liver or cells was extracted using Direct-zol RNA MiniPrep (cat. no. R2050; Zymo Research, Irvine, CA) or the RNeasy Mini Kit (cat. no. 74104; Qiagen, Hilden, Germany).

cDNA libraries for all samples were created using the TruSeq RNA Sample Prep Kit v2–48, Set A (cat. no. RS-122-2001; Illumina, San Diego, CA) and Set B (cat. no. RS-122-2002; Illumina). For specifics, see Supplementary Materials.

Alignment, Analysis of Technical Performance, and Bioinformatics

The cDNA libraries were sequenced on a HiSeq 2000 with a 50–52 read length, single-end, for different samples.[17] Bioinformatics and sequencing details are provided in Supplementary Materials.

Human Protein Atlas Cross-referencing Enrichment of Bile Duct Genes

Proteins expressed in bile ducts were identified using the Human Protein Atlas (HPA, http://www.proteinatlas.org/),[18] using the following search string: Field: Tissue expression (IHC), Tissue: Liver, Cell Type: Bile duct cells, Expression: High or Medium AND Field: Tissue expression (IHC), Tissue: Liver, Cell Type: Bile duct cells, Expression: Not detected or low. Supplementary Tables 5–8. For details, see Supplementary Materials.

Bile Duct Orientation by ZO-1 Staining in Adult Mice

ZO-1 orientation analysis was carried out in 6–12 well-formed/functional bile ducts per animal (n=3).

IGF1 ELISA

IGF1 in serum was detected using ELISA according to manufacturer's instructions (cat. no. EMIGF1; Thermo Fisher Scientific, Waltham, MA).

Cell Lines and Cell Culture

Mouse C2C12 control and C2C12-*FLNotch1* and human HEK-293-Flp-In cells[8]: HEK293-Flp control (Flp Ctrl), HEK293-Flp-$Jag1^{WT}$ (Flp JAG1^{+}), HEK293-Flp-$Jag1^{Ndr}$ (Flp JAG1^{Ndr}) were used. For culture conditions and luciferase experiments, see Supplementary Materials.

Notch ECD Uptake Experiments

NOTCH1-Fc, NOTCH2-Fc, and NOTCH3-Fc (R&D Systems, Minneapolis, MN) was coupled to Alexa 488 anti-Fc (Invitrogen, Carlsbad, CA). Flp Ctrl, Flp JAG1^{+}, and Flp JAG1^{Ndr} cells were treated with the tagged proteins for 1 hour at 37°C. Cells were stained for confocal imaging or trypsinized for fluorescence-activated cell sorter fluorescence-activated cell sorting (FACS) analysis, as described in Supplementary Materials.

Statistical Analysis

Differences between control and experimental conditions were tested using *t* test, 1-way ANOVA, or 2-way ANOVA. For specifics, see Supplementary Materials.

Results

$Jag1^{Ndr/Ndr}$ Mice Recapitulate Alagille Syndrome

We previously described a mouse *Jag1* mutation (H268Q) in the second epidermal growth factor (EGF)-like repeat of JAG1,[8] a region enriched for missense mutations in ALGS.[1] This allele is nicknamed Nodder ($Jag1^{Ndr}$) because of a head-nodding phenotype in heterozygous C3H mice. $Jag1^{Ndr/Ndr}$ mice are embryonic lethal on this genetic background[8] and, because the phenotype of other *Jag1* heterozygous mice depends on genetic background,[14,19] we asked whether mixed $Jag1^{Ndr/Ndr}$ mice bypass C3H lethality and recapitulate ALGS.

On a mixed C3H/C57bl6 background, viability was considerably improved: $Jag1^{Ndr/Ndr}$ embryos were recovered at a rate of 20% at embryonic day (E) 15.5, 10% from postnatal day

(P) 0, and 5% in adults (Figure 1*A*, Supplementary Table 1, and data not shown). At E15.5, *Jag1*$^{Ndr/Ndr}$ embryos appeared grossly normal, and only exhibited a mild iris dysmorphology (Figure 1*B*). In contrast, postnatal *Jag1*$^{Ndr/Ndr}$ pups were jaundiced (Figure 1*C*), excreted yellow stools (data not shown), exhibited partial post-natal mortality (Figure 1*D*), and failed to thrive (Figure 1*E*). Adult *Jag1*$^{Ndr/Ndr}$ mice were 30% smaller than *Jag1*$^{+/+}$ and *Jag1*$^{+/Ndr}$ mice (Figure 1*F*).

ALGS is diagnosed based on the presence of cholestasis, ocular abnormalities, characteristic facial features, heart defects, and vertebral malformations.[6] The heart defects range from pulmonary artery stenosis to tetralogy of Fallot, a severe defect encompassing pulmonary stenosis, overriding aorta, ventricular septal defect, and right ventricular hypertrophy.[20] Both atrial and ventricular septation defects were present in E15.5 and P0 *Jag1*$^{Ndr/Ndr}$ mice (Figure 1*G* and Supplementary Figure 1*A*).

Patients with ALGS display posterior embryotoxon,[12] a malformation attributed to neural crest defects,[21] and a smaller cornea.[22] The first obvious phenotype in *Jag1*$^{Ndr/Ndr}$ mice was bilateral iris deformation with dorsal constriction at E13.5, which progressed to severe deformities and occasionally micropthalmia by P10 (Figure 1*B,H,* and Supplementary Figure 1*B*). *Jag1*$^{Ndr/Ndr}$ lenses were similar to wild types in size at E15.5 and were only slightly smaller at P10 (Supplementary Figure 1*C,D*), while 30% of adult *Jag1*$^{Ndr/Ndr}$ mice exhibited micropthalmia (data not shown).

Craniofacial alterations, including a broad prominent forehead, deep-set eyes, and a pointy chin, are seen in 77%–96% of patients.[12] *Jag1*$^{Ndr/Ndr}$ mice similarly displayed a tendency toward altered craniofacial proportions with a wild type eye-nose length (Figure 1*I,J*), but a reduced snout length (bridge to tip, Figure 1*I,K*), supporting a role for Jag1 in craniofacial development, in line with previous reports.[23] Alcian blue/Alizarin red staining of cartilage and bone at P0 and P10 did not reveal obvious vertebral malformations (data not shown), indicating that butterfly vertebrae[12] are probably not present in *Jag1*$^{Ndr/Ndr}$ mice.

In conclusion, *Jag1*$^{Ndr/Ndr}$ mice recapitulate cardinal features of ALGS, including ocular, craniofacial, and cardiac defects. Jaundice indicates liver dysfunction, and we therefore next asked whether *Jag1*$^{Ndr/Ndr}$ mice display ductopenia.

Jag1$^{Ndr/Ndr}$ Mice Exhibit Early Life Biliary Dysmorphogenesis and Dysfunction With Later Rescue

A crippling ALGS symptom is cholestatic liver disease, with conjugated hyperbilirubinemia and decreased liver function, which histologically is associated with paucity of intrahepatic bile ducts. Thus, liver transplantation is frequently required. The pathomechanisms for ductopenia are poorly understood and it is unclear why, in some patients, cholestasis diminishes with time.[24,25] Because some *Jag1*$^{Ndr/Ndr}$ mice survive to adulthood, the model provides an opportunity to elucidate disease development across different stages.

Jag1$^{Ndr/Ndr}$ mice displayed strong jaundice at neonatal stages (Figure 1*C*), whereas surviving adult *Jag1*$^{Ndr/Ndr}$ mice did not display jaundice, nor excrete yellow feces (data not shown). To determine whether *Jag1*$^{Ndr/Ndr}$ mice manifest a transient biliary phenotype, we

analyzed biliary histology and marker expression in portal regions during development. Both Sox9 (a Notch target gene that regulates bile duct development[26]) and Hnf1β were present in *Jag1*$^{+/+}$ periportal areas, but absent in *Jag1*$^{Ndr/Ndr}$ mice at E18.5. At p0, faintly positive cells were detected around portal tracts in *Jag1*$^{Ndr/Ndr}$ mice, at levels far weaker than the clusters of Sox9/Hnf1β-positive cells undergoing lumen formation in *Jag1*$^{+/+}$ livers. At this stage, *Jag1*$^{Ndr/Ndr}$ hilar portal regions had no morphologically discernible mature bile ducts, while 3.3% of *Jag1*$^{+/+}$ hilar portal veins had adjoining mature bile ducts (Figure 2*C,D*). The majority of P0 portal veins in *Jag1*$^{Ndr/Ndr}$ livers contained either no KRT19+ cells or disorganized clusters of KRT19+ cells (Figure 2*B–D*, Supplementary Figure 2*A*). At P10, bile ducts were rarely found in *Jag1*$^{Ndr/Ndr}$ livers, while portal veins in *Jag1*$^{+/+}$ livers manifested 1 or 2 adjacent mature bile ducts (Figure 2*E,F*; Supplementary Figure 2*B,C*). Hepatoblast and hepatocyte marker expression levels were unaltered (data not shown), but serum biochemistry at P10 confirmed that *Jag1*$^{Ndr/Ndr}$ liver function was severely compromised (Figure 2*G–J*, Supplementary Figure 2*D–F*).

In contrast, lumenized bile ducts could be found in both *Jag1*$^{+/+}$ and *Jag1*$^{Ndr/Ndr}$ adult mice, though with disrupted morphology in *Jag1*$^{Ndr/Ndr}$ livers (Figure 2*K–M*, Supplementary Figure 2*G,H*). We classified and quantified pan-cytokeratin+ and KRT19+ bile ducts as “well-formed” (1 layer of biliary cells, a round lumen), “functional” (1 or more layers of biliary cells, a discernible lumen) or “clusters” (clusters of biliary cells, no discernible lumen) (Figure 2*L*). Adult *Jag1*$^{Ndr/Ndr}$ mice harbor fewer “well-formed” bile ducts and instead contain “clusters” of biliary cells (Figure 2*M*, Supplementary Figure 2*G*). However, there was no significant difference between *Jag1*$^{+/+}$ and *Jag1*$^{Ndr/Ndr}$ mice when grouping well-formed and functional bile ducts (Supplementary Figure 2*H*). Serum analysis confirmed a full functional recovery in adult *Jag1*$^{Ndr/Ndr}$ mice (Figure 2*N*, Supplementary Figure 2*I,J*), with only a small difference in aspartate aminotransferase levels still detectable.

In contrast to the transient biliary phenotype, there was a persistent absence of hepatic arteries in *Jag1*$^{Ndr/Ndr}$ mice (Figure 2*K*, Supplementary Figure 2*K,L*). In conclusion, the *Jag1*$^{Ndr/Ndr}$ mice display a biliary phenotype that is severe at early postnatal stages but that improves during adulthood.

Disrupted Bile Duct Morphogenesis and Delayed Differentiation

It is unclear whether the ALGS biliary defects are because of disrupted morphogenesis,[11] differentiation defects,[27] or both.[28] To address this question, we analyzed the expression of key genes regulating differentiation. Expression of *Sox9*, and *Hnf4α*, a transcription factor required for hepatocyte differentiation,[29] as well as alfa-fetoprotein (a marker of hepatoblasts) and albumin (a marker for hepatocyte function), was unaffected in P10 and adult *Jag1*$^{Ndr/Ndr}$ mice (Figure 3*A–F*, data not shown). Similarly, *SOX9* mRNA levels were not affected in ALGS liver biopsies (Figure 3*G*), nor were the well-characterized biliary markers *HNF1β* or *KRT19* (Figure 3*H,I*). This is in contrast to the early absence of SOX9- and HNF1β-positive cells at E18.5 and P0 (Figure 2*A,B*).

To assess adult bile duct development and morphology, we used a recently developed model for long-term in vitro expansion of bile duct-derived progenitor cells.[16,30] Bile duct fragments were hand-picked and cultured in vitro as liver organoids, forming readily from

both adult control and *Jag1*$^{Ndr/Ndr}$ mice. *Notch2*, *Hes1*, *Hnf4α*, *Sox9,* and *Hnf1β* mRNA expression were not altered (Figure 3*J–N*), further supporting that differentiation was delayed, but not completely inhibited (see Figure 2). However, liver organoids from *Jag1*$^{Ndr/Ndr}$ mice grew less well than *Jag1*$^{+/+}$ organoids (Figure 3*O*). Importantly, a number of *Jag1*$^{Ndr/Ndr}$ organoids collapsed in culture after 5–6 days (Figure 3*P*), demonstrating structural instability. *Jag1*$^{Ndr/Ndr}$ biliary cells from adult mice are therefore similar to *Jag1*$^{+/+}$ biliary cells in terms of cell identity, but exhibit differences in structural stability. In conclusion, the data argue for morphologic as well as differentiation defects.

Novel Biomarkers for Alagille Syndrome Reveal Dysregulation of Apical Proteins

To further assess the molecular basis for ALGS, we performed genome-wide transcriptome studies of liver biopsies from 5 patients with ALGS. Control samples from pediatric patients with liver disease and/or cholangiopathies allow us to detect genes specifically dysregulated in ALGS, rather than cholestasis pathways or general liver disease mechanisms. Principal component analysis (PCA) showed that the 5 ALGS liver transcriptomes clustered with the 2 cholangiopathy samples: autoimmune hepatitis with primary sclerosing cholangitis, and progressive familial intrahepatic cholestasis type 2. In contrast, the transcriptomes from 2 patients with autoimmune hepatitis segregated more distinctly (Figure 4*A*, Supplementary Table 2). There were 191 up-regulated and 139 down-regulated genes (adjusted *P* value <.1, fold change >1.5, Figure 4*B*, Supplementary Tables 3 and 4, Supplementary Figure 3).

The transcriptome data are derived from bulk liver. We therefore devised a strategy to cross-reference the transcriptome data with protein expression patterns from the HPA (http://www.proteinatlas.org), a map of the human proteome,[18] allowing us to identify genes encoding proteins expressed in bile ducts (Figure 4*C*, Supplementary Tables 5–8). This strategy identified the well-established biliary markers HNF1β, KRT19, and SOX9, confirming strategy validity and specificity, and HPA data showed the expected biliary expression (Supplementary Figure 4*A*).

Comparison of HPA bile duct-enriched proteins to ALGS transcriptomes revealed 5 up-regulated and 7 down-regulated novel bile duct markers in ALGS (Figure 4*D,E*, Supplementary Figure 4*B–L*). Of these, *FXYD domain containing ion transport regulator 3* (*FXYD3*, Figure 4*D*) and *Solute carrier family 5 (sodium/glucose cotransporter) member 1* (*SLC5A1*, Figure 4*E*) showed the highest significance, and encode proteins enriched at the apical surface of bile ducts. Manual comparison of the protein localization of the top 30 down-regulated genes to the HPA revealed 5 additional bile duct-specific genes with apical cholangiocyte staining including *Cystic Fibrosis Transmembrane Conductance Regulator* (*CFTR*, Figure 4*F*), *Carbohydrate Sulfotransferase 4* (*CHST4*, Figure 4*G*), *Claudin 10* (*CLDN10*, Figure 4*H*), *Interleukin 1 receptor-like 1* (*IL1RL1*, Figure 4*I*) and *Solute Carrier Family 6 (Neutral Amino Acid Transporter) member 19* (*SLC6A19*, Figure 4*J*). Given this link to aberrant cell polarity, we assessed the distribution of Zona occludens 1 (ZO-1, a.k.a. TJP-1), a marker of apical junctions in cholangiocytes that is not down-regulated in ALGS or in *Jag1*$^{Ndr/Ndr}$ mice (data not shown). Even in the best-formed bile ducts in *Jag1*$^{Ndr/Ndr}$ mice, ZO-1 was mis-localized, confirming polarity defects (Figure 4*K–M*). In conclusion,

the most highly down-regulated biliary genes encode proteins enriched at the apical surface of bile ducts, corroborating morphogenesis disruption in ALGS.

Igf1 is Down-regulated in Patients With ALGS and *Jag1*$^{Ndr/Ndr}$ Mice

We next compared the transcriptomic changes in *Jag1*$^{Ndr/Ndr}$ livers to ALGS livers. RNA sequencing of *Jag1*$^{Ndr/Ndr}$ and *Jag1*$^{+/+}$ livers yielded distinct transcriptional profiles (Figure 5*A*, Supplementary Table 9), with 679 up-regulated and 374 down-regulated genes (Figure 5*B*, Supplementary Tables 10 and 11, and Supplementary Figure 5).

We assessed changes in signaling pathways and major cellular programs using gene set enrichment analyses (GSEA), which identified 35 sets significantly enriched in *Jag1*$^{Ndr/Ndr}$ livers at False Discovery Rate <25% (Figure 5*C*, Supplementary Tables 12 and 13, GSEA in Supplementary Figure 6). In contrast, GSEA for the ALGS transcriptome showed 6 enriched gene sets (Supplementary Tables 14 and 15, Supplementary Figure 7).

We next examined genes that were up- or down-regulated in both ALGS livers and in *Jag1*$^{Ndr/Ndr}$ livers. Sixteen genes were up-regulated (Figure 5*D*) and 2 were down-regulated (Figure 5*E*) in both transcriptomes. This relatively small degree of overlap is likely explained by the use of different controls in the 2 experiments (non-ALGS liver pathologies for patient data, and *Jag1*$^{+/+}$ for mouse data), and innate differences between humans and mice, as well as in age. To test whether the use of different controls revealed different aspects of disease, we compared ALGS liver transcriptomes with the cholangiopathic and non-cholangiopathic controls separately (Supplementary Figure 8*A*–*C*). A greater numbers of enriched gene sets and dysregulated genes were detected when ALGS livers were compared with non-cholangiopathic livers (Supplementary Figure 8*D*–*G*, Supplementary Tables 16–19), than when ALGS livers were compared with cholangiopathic livers (Supplementary Figure 8*H*–*K*, Supplementary Tables 20–23), indicating general cholangiopathic transcriptomic responses are additionally revealed when non-cholestatic patients are included as controls. This is corroborated by the higher general overlap of this dataset with the *Jag1*$^{Ndr/Ndr}$ results (Supplementary Figure 8*D*–*K*). In all analyses, *Igf1* (*Insulin like growth factor 1*) emerges as a target of particular interest.

Down-regulation of *Igf1* in ALGS and in *Jag1*$^{Ndr/Ndr}$ mice is in line with a previous report showing that IGF1 is not up-regulated upon administration of growth hormone to patients with ALGS and growth deficiencies.[31] The reduced expression of *Igf1* in patients (Figure 5*F*) and in *Jag1*$^{Ndr/Ndr}$ mice (Figure 5*G*), which we confirmed with ELISA of serum from P10 and adult *Jag1*$^{Ndr/Ndr}$ mice (Figure 5*H,I*), is also likely to explain the *Jag1*$^{Ndr/Ndr}$ growth defects (Figure 1*C,E,F*).

JAG1^{Ndr} Elicits Hypomorphic Notch Signaling

To address how the JAG1^{Ndr} mutation influences signaling downstream of Notch, we analyzed the genome-wide transcriptomic response in NOTCH-expressing cells following activation by JAG1^{+} or JAG1^{Ndr}. To specifically monitor the Notch response, we co-cultured mouse receptor cells (C2C12) with human ligand cells (HEK293 Flp) (Figure 6*A*). The transcriptome of C2C12 cells was bioinformatically separated from the HEK293 transcriptome based on species-specific sequencing (S^3, Figure 6*B*, Supplementary Figure

9), which separates more than 99% of a mixed transcriptome to the correct species.[17] Notch target gene responses were specifically detectable in the Notch receptor-expressing (mouse) cell reads in conditions with Notch activation (Figure 6*C–F*, Supplementary Figure 10*A–D*).

We co-cultured ligand-expressing HEK293 Flp cells with control C2C12 cells (which express *Notch2* and *Notch3* at twice the levels of *Notch1* and with almost undetectable *Notch4* [Supplementary Figure 10*E*]), or with NOTCH1-overexpressing C2C12 cells, to examine whether NOTCH1 modified the transcriptomic response induced by ligand-expressing cells. PCA of the mouse transcriptomes showed that the JAG1^{Ndr}-induced transcriptome is intermediate between response to control cells, and response to JAG1^{+}-expressing cells (Figure 6*G*, Supplementary Table 24). However, in C2C12 cells, which predominantly express *Notch2* and *Notch3*, the JAG1^{Ndr}-induced transcriptome clustered with the JAG1^{+}-induced transcriptome, whereas for NOTCH1-overexpressing C2C12 cells, the JAG1^{Ndr} transcriptome lay closer to the Ctrl-induced transcriptome. This suggests that JAG1^{Ndr} signals weakly or not at all through NOTCH1, in line with our previous report.[8] In addition, Notch target genes showed weak (10%–80%) up-regulation by the JAG1^{Ndr} ligand (Supplementary Figure 10*F*). In sum, the JAG1^{Ndr} allele is hypomorphic at the global transcriptome level with regard to its ability to elicit Notch signaling.

JAG1^{Ndr} Induces Receptor-selective Binding

The differentially hypomorphic signaling elicited by JAG1^{Ndr} suggested that JAG1^{Ndr}-mediated signaling through Notch receptor paralogs may be altered. Because the H268Q mutation resides in the Notch receptor-interacting domain, we tested whether JAG1^{Ndr} exhibited receptor paralog-specific binding. Flp JAG1^{+} or Flp JAG1^{Ndr} ligand-expressing cells were treated with fluorescently tagged soluble NOTCH1-3 receptor extracellular domain peptides (N1-3ECD, Figure 6*H*). Immunocytochemistry for the NECD-Fc was performed, without permeabilization, to detect extracellular ECDs (Figure 6*H*). N2ECD and N3ECD were bound by Flp JAG1^{+} and Flp JAG1^{Ndr} cells, whereas N1ECD only interacted with Flp Jag1^{+} (Figure 6*H*); the latter in keeping with our previous report.[8] FACS analysis showed that N1ECD was internalized by 50% of Flp JAG1^{+} cells, while Flp JAG1^{Ndr} cells did not significantly internalize N1ECD (Figure 6*I–L*, Supplementary Figure 10*G*). In contrast, N2ECD was internalized by 80% of Flp JAG1^{+} cells, and by 70% of Flp JAG1^{Ndr} cells (Figure 6*M–P*). However, the amount of N2ECD internalized by Flp JAG1^{Ndr} cells was lower than by Flp JAG1^{+} cells (Supplementary Figure 10*H*). N3ECD was internalized by 35% of Flp Jag1^{+} cells, and by 20% of Flp Jag1^{Ndr} cells (Figure 6*Q–T*, Supplementary Figure 10*I*). Because N2ECD internalization was reduced, we next tested the extent of activation of cells expressing Notch2 receptors, in response to co-culture with cells expressing Flp JAG1^{+} or Flp JAG1^{Ndr}. Co-culture with Flp JAG1^{Ndr} cells resulted in reduced Notch activation (as defined by 12XCSL-luciferase activation), as compared with co-culture with Flp JAG1^{+} cells (Supplementary Figure 10*J*). In conclusion, Flp JAG1^{Ndr} exhibits a selective loss of interaction with NOTCH1, but the interaction with NOTCH2 and NOTCH3 is partially retained, although NOTCH2-mediated signaling elicited by Flp JAG1^{Ndr} is reduced.

Discussion

ALGS is usually caused by mutations in the *JAG1* gene, but how dysregulated Notch signaling links to phenotypic consequences has been enigmatic. In this report, we provide evidence that a *Jag1* missense mutation ($Jag1^{H268Q}$) recapitulates Alagille symptoms in a number of organs. $Jag1^{H268Q}$ elicits a reduced Notch transcriptomic response and Notch receptor-selective binding (schematically depicted in Figure 7).

Disturbed Morphogenesis in $Jag1^{Ndr}$ Bile Ducts

The $Jag1^{Ndr/Ndr}$ mouse demonstrates that a *Jag1* missense mutation can recapitulate ALGS. Other models based on loss-of-function *Jag1* and/or *Notch2* alleles do not display the entire spectrum of disease phenotypes. The $Jag1^{Ndr/Ndr}$ mouse displays Alagille-like phenotypes in several organs, including heart, lens, and craniofacial structures, as well as liver, and thus represents a clinically relevant mouse model for ALGS. An important distinction must be made, however, with regards to genetics: ALGS in humans is generally caused by heterozygosity for *JAG1*, while in mice the phenotype arises in the homozygous $Jag1^{Ndr/Ndr}$ state.

The fact that $Jag1^{Ndr/Ndr}$ mice survive to adulthood provides an opportunity to explore liver pathology over a lifetime. Interestingly, despite neonatal ductopenia, the number of bile ducts increases in the adult – although with aberrant morphology. In keeping with this, cholestasis was pronounced in pups, while adults display a full recovery regarding cholestasis, suggesting compensatory mechanisms rescue ductopenia in $Jag1^{Ndr/Ndr}$ mice. To what extent recuperation of the liver occurs also in ALGS is contested because some patients recover from cholestasis with time[32] while in others biliary breakdown continues.[24,25] Some patients display regenerating liver nodules with normal bile duct numbers.[24,33,34] The RNA sequencing of ALGS liver samples (Figure 4) showed some heterogeneity, and in light of the variable liver disease severity and progression or reversal, additional analyses on bigger cohorts of patients will be necessary to determine whether there is a unifying molecular mechanism leading to bile duct abnormalities and whether diseases progression can be predicted based on transcriptomic data. The notion of a transient liver phenotype is also of interest for therapy; if cholestasis could be temporarily treated, then harnessing endogenous repair mechanisms could reduce the need for liver transplantation. In this context, the $Jag1^{Ndr/Ndr}$ mouse may serve as an important tool to explore novel therapeutic strategies, to test if transplanted cells can give rise to bile ducts, or which treatments induce repair mechanisms.

The $Jag1^{Ndr/Ndr}$ mice also shed light on the nature of the ALGS biliary pathology, attributed to disrupted morphogenesis of the bile ducts,[11] defective bile duct maintenance, or differentiation defects.[27,28] Our data indicate that morphogenesis and maintenance of bile ducts are affected, in addition to differentiation. This notion is supported by profound changes in gene expression in ALGS affecting cell polarity, at postnatal and adult stages. Further support for disturbed morphogenesis comes from the liver organoid data, in which $Jag1^{Ndr/Ndr}$ organoids initiated growth but collapsed a few days later, supporting structural rather than developmental defects. A previous report showed that liver organoids from

human Alagille livers showed no phenotype in the undifferentiated state, but underwent collapse and apoptosis upon R-spondin withdrawal.[30]

Dysregulated cell polarity by disrupted Notch signaling has been shown in other polarized structures. Removal of *CSL*, the canonical Notch transcription factor, in embryonic stem cells disrupts neural rosettes,[35] a lumenized and polarized colony of neural cells modeling the neural tube in vitro. Similarly, in the zebrafish lateral line, Notch is required for apical constriction of proneuromast rosettes,[36] and regulates apical junction-associated genes, which together with our results, indicates a more general interaction between Notch and the cell polarity machinery.

The Jag1^{Ndr} Mutation Causes Hypomorphic Signaling and Receptor Selectivity

Our data lend support to the hypomorphic view of ALGS mutations. The transcriptome data from co-cultured ligand- and receptor-expressing cells indicate that Jag1^{Ndr} induces a hypomorphic Notch signaling response.

The finding that the H268Q mutation yields a JAG1 ligand that selectively loses its ability to interact with and activate NOTCH1, while maintaining interaction with NOTCH2 and 3, provides a novel facet of Notch signaling. Modifications of NOTCH receptors by Fringe fine-tunes their interaction with JAG or DLL ligands, but that a ligand mutation is sufficient to select for NOTCH2 and 3, but not NOTCH1, interaction is unprecedented. The H268Q missense mutation falls in the second EGF repeat, a region involved in Notch receptor activation,[37] close to a number of patient-specific *JAG1* mutations,[1] and close to 3 interacting amino acids in NOTCH1, in EGF9, and EGF10,[7] 2 of which are conserved in NOTCH2 (L368 and P391); whereas the Valine 392 in NOTCH1 is instead a Leucine in NOTCH2. Whether this difference will explain the differential effect of the JAGGED1 H268Q mutation on NOTCH1 and 2 activation, however, remains to be tested. This difference cannot explain differences in binding to NOTCH3 because all 3 amino acids are conserved in NOTCH3 (Supplementary Materials).

The Recovery of *Jag1$^{Ndr/Ndr}$* Mice Suggests Endogenous Mechanisms can Rescue Alagille Syndrome

Why certain patients with ALGS recover liver biliary function while others progress to liver transplantation is currently unknown. *Jag1$^{Ndr/Ndr}$* pups display a severe biliary phenotype that is functionally rescued in adults. This is in contrast to *Jag1$^{+/dDSL}$* mice, which display ALGS-like liver phenotypes in a C57bl6 background, but are not reported to improve with age.[14]

Sox9 is expressed not only in cholangiocytes, but also in stem-like hepatocytes upon insult,[9,38,39] which can trans-differentiate into cholangiocytes. A similar rescue in adult albumin-Cre Hnf6$^{flox/flox}$ Rbpj$^{flox/flox}$ mice[40] suggests Notch-independent mechanisms induce ductular reaction and hepatocyte trans-differentiation. The recovery in *Jag1$^{Ndr/Ndr}$* mice may also be because of hepatocyte trans-differentiation, which can be induced with Notch activation.[28] Thus, although Notch is not required for rescue, it may be sufficient. Transient activation of Notch may therefore – in principle – be feasible as therapy, though the role of Notch signaling in cancer suggests this could be associated with significant risks.[41,42] The

loss of *Igf1* also presents an interesting therapeutic target because Igf1 stimulates cholangiocyte proliferation.[43]

While *Jag1*$^{Ndr/Ndr}$ mice recovered biliary function they did not recover hepatic artery numbers, suggesting that the absence of proper portal triad vascular architecture does not preclude recovery of a functional biliary tree. Thus, cholangiocytes are not completely dependent on the presence of a hepatic artery, which would otherwise be suggested by the biliary breakdown induced by hepatic artery ligation, and which would preclude cell replacement therapy. Instead, our results suggest cell replacement therapies to replace absent cholangiocytes may be feasible, even in the absence of normal hepatic vasculature.

Our data, showing a selective loss of primarily Notch1-mediated signaling, may be at apparent odds with the fact that ALGS can be caused by *NOTCH2* mutations,[12] and that compound heterozygous *Jag1*/*Notch2* mice are also growth delayed, display jaundice, and recapitulate hepatic, cardiac, renal, and ocular defects.[10] Moreover, Notch2 is required for bile duct morphogenesis and differentiation in vivo, [44–46] while Notch1 is dispensable.[44] However, the mildly reduced Jag1^{Ndr}-Notch2 signaling described here may be sufficient to cause a pathologic outcome in keeping with the dose-sensitive nature of the Notch signaling pathway.

In sum, the Nodder mouse provides a clinically relevant model for ALGS and allows for the first time a *Jag1* missense mutation to be linked both to phenotypic traits typical for the disease and to dysregulated Notch signaling, manifested by hypomorphic signaling and receptor-selectivity.

Supplementary Material

Refer to Web version on PubMed Central for supplementary material.

Acknowledgments

Funding

U.L. acknowledges support from the Swedish Research Council (project grant and the Linnaeus Center DBRM), European Research Council Marie Curie ITN-FP7 NotchIT (IVC), the Swedish Cancer Society, Hjärnfonden, Knut och Alice Wallenbergs Stiftelse, and ICMC (the Integrated Cardio Metabolic Center). E.R.A. and members of Andersson lab were supported by a Center of Innovative Medicine (CIMED) Grant, the Daniel Alagille Award, KI Funding, and the Alex and Eva Wallström Foundation. S.H. was supported by Wera Ekströms Stiftelse and a grant for KI-MU exchange (see below), and grants in ERA lab. M.S. was supported by an OSK Huttunen post doc fellowship. J.M. was supported by a WennerGren Fellowship and grants in ERA lab. V.B. and S.H. were supported by “KI-MU” program (CZ.1.07/2.3.00/20.0180) co-financed from European Social Fund and the state budget of the Czech Republic.

The funders had no role in study design, analysis, or interpretation of data.

Abbreviations used in this paper

ALGS	Alagille syndrome
ECD	extracellular domain
EGF	epidermal growth factor

FACS	fluorescence-activated cell sorting
GSEA	gene set enrichment analyses
HPA	Human Protein Atlas
PCA	principal component analysis
qPCR	quantitative real-time polymerase chain reaction

References

1. Mašek J, Andersson ER. The developmental biology of genetic Notch disorders. Development. 2017; 144:1743–1763. [PubMed: 28512196]
2. Grochowski CM, Loomes KM, Spinner NB. Jagged1 (JAG1): structure, expression, and disease associations. Gene. 2016; 576:381–384. [PubMed: 26548814]
3. Li L, Krantz ID, Deng Y, et al. Alagille syndrome is caused by mutations in human Jagged1, which encodes a ligand for Notch1. Nat Genet. 1997; 16:243–251. [PubMed: 9207788]
4. Oda T, Elkahloun AG, Pike BL, et al. Mutations in the human Jagged1 gene are responsible for Alagille syndrome. Nat Genet. 1997; 16:235–242. [PubMed: 9207787]
5. McDaniell R, Warthen DM, Sanchez-Lara PA, et al. NOTCH2 mutations cause Alagille syndrome, a heterogeneous disorder of the notch signaling pathway. Am J Hum Genet. 2006; 79:169–173. [PubMed: 16773578]
6. Alagille D, Odièvre M, Gautier M, et al. Hepatic ductular hypoplasia associated with characteristic facies, vertebral malformations, retarded physical, mental, and sexual development, and cardiac murmur. J Pediatr. 1975; 86:63–71. [PubMed: 803282]
7. Luca VC, Kim BC, Ge C, et al. Notch-Jagged complex structure implicates a catch bond in tuning ligand sensitivity. Science. 2017; 1:1–24.
8. Hansson EM, Lanner F, Das D, et al. Control of Notch-ligand endocytosis by ligand-receptor interaction. J Cell Sci. 2010; 123:2931–2942. [PubMed: 20720151]
9. Hofmann JJ, Zovein AC, Koh H, et al. Jagged1 in the portal vein mesenchyme regulates intrahepatic bile duct development: insights into Alagille syndrome. Development. 2010; 137:4061–4072. [PubMed: 21062863]
10. McCright B, Lozier J, Gridley T. A mouse model of Alagille syndrome: Notch2 as a genetic modifier of Jag1 haploinsufficiency. Development. 2002; 129:1075–1082. [PubMed: 11861489]
11. Lozier J, McCright B, Gridley T. Notch signaling regulates bile duct morphogenesis in mice. PLoS One. 2008; 3:e1851. [PubMed: 18365007]
12. Spinner, NB, Leonard, LD, Krantz, ID. Alagille Syndrome. University of Washington; Seattle: 2013.
13. Kamath BM, Bauer RC, Loomes KM, et al. NOTCH2 mutations in Alagille syndrome. J Med Genet. 2012; 49:138–144. [PubMed: 22209762]
14. Thakurdas SM, Lopez MF, Kakuda S, et al. Jagged1 heterozygosity in mice results in a congenital cholangiopathy which is reversed by concomitant deletion of one copy of Poglut1 (Rumi). Hepatology. 2016; 63:550–565. [PubMed: 26235536]
15. Jin S, Mutvei AP, Chivukula IV, et al. Non-canonical Notch signaling activates IL-6/JAK/STAT signaling in breast tumor cells and is controlled by p53 and IKKα/IKKβ. Oncogene. 2013; 32:4892–4902. [PubMed: 23178494]
16. Huch M, Dorrell C, Boj SF, et al. In vitro expansion of single Lgr5+ liver stem cells induced by Wnt-driven regeneration. Nature. 2013; 494:247–250. [PubMed: 23354049]
17. Chivukula IV, Ramsköld D, Storvall H, et al. Decoding breast cancer tissue-stroma interactions using species-specific sequencing. Breast Cancer Res. 2015; 17:109. [PubMed: 26265142]
18. Uhlen M, Oksvold P, Fagerberg L, et al. Towards a knowledge-based Human Protein Atlas. Nat Biotechnol. 2010; 28:1248–1250. [PubMed: 21139605]

19. Kiernan AE, Li R, Hawes NL, et al. Genetic background modifies inner ear and eye phenotypes of Jag1 heterozygous mice. Genetics. 2007; 177:307–311. [PubMed: 17890364]
20. McElhinney DB, Krantz ID, Bason L, et al. Analysis of cardiovascular phenotype and genotype-phenotype correlation in individuals with a JAG1 mutation and/or Alagille syndrome. Circulation. 2002; 106:2567–2574. [PubMed: 12427653]
21. Williams AL, Bohnsack BL. Neural crest derivatives in ocular development: discerning the eye of the storm. Birth Defects Res C Embryo Today. 2015; 105:87–95. [PubMed: 26043871]
22. Kim BJ, Fulton AB. The genetics and ocular findings of Alagille syndrome. Semin Ophthalmol. 2007; 22:205–210. [PubMed: 18097983]
23. Humphreys R, Zheng W, Prince LS, et al. Cranial neural crest ablation of Jagged1 recapitulates the craniofacial phenotype of Alagille syndrome patients. Hum Mol Genet. 2012; 21:1374–1383. [PubMed: 22156581]
24. Jinguji M, Tsuchimochi S, Nakajo M, et al. Scintigraphic progress of the liver in a patient with Alagille syndrome (arteriohepatic dysplasia). Ann Nucl Med. 2003; 17:693–697. [PubMed: 14971613]
25. Sparks EE, Perrien DS, Huppert KA, et al. Defects in hepatic Notch signaling result in disruption of the communicating intrahepatic bile duct network in mice. Dis Model Mech. 2011; 4:359–367. [PubMed: 21282722]
26. Antoniou A, Raynaud P, Cordi S, et al. Intrahepatic bile ducts develop according to a new mode of tubulogenesis regulated by the transcription factor SOX9. Gastroenterology. 2009; 136:2325–2333. [PubMed: 19403103]
27. Tanimizu N, Miyajima A. Notch signaling controls hepatoblast differentiation by altering the expression of liver-enriched transcription factors. J Cell Sci. 2004; 117:3165–3174. [PubMed: 15226394]
28. Zong Y, Panikkar A, Xu J, et al. Notch signaling controls liver development by regulating biliary differentiation. Development. 2009; 136:1727–1739. [PubMed: 19369401]
29. Li J, Ning G, Duncan SA. Mammalian hepatocyte differentiation requires the transcription factor HNF-4alpha. Genes Dev. 2000; 14:464–474. [PubMed: 10691738]
30. Huch M, Gehart H, Van Boxtel R, et al. Long-term culture of genome-stable bipotent stem cells from adult human liver. Cell. 2015; 160:299–312. [PubMed: 25533785]
31. Bucuvalas JC, Horn JA, Carlsson L, et al. Growth hormone insensitivity associated with elevated circulating growth hormone-binding protein in children with Alagille syndrome and short stature. J Clin Endocrinol Metab. 1993; 76:1477–1482. [PubMed: 8501153]
32. Riely CA, Cotlier E, Jensen PS, et al. Arteriohepatic dysplasia: A benign syndrome of intrahepatic cholestasis with multiple organ involvement. Ann Intern Med. 1979; 91:520–527. [PubMed: 484950]
33. Torizuka T, Tamaki N, Fujita T, et al. Focal liver hyperplasia in Alagille syndrome: assessment with hepatoreceptor and hepatobiliary imaging. J Nucl Med. 1996; 37:1365–1367. [PubMed: 8708775]
34. Tuset E, Ribera JM, Doménech E, et al. Pseudotumorous hyperplasia of the caudate lobe of the liver in a patient with Alagille syndrome. Med Clin (Barc). 1995; 104:420–422. [PubMed: 7715262]
35. Main H, Radenkovic J, Jin SB, et al. Notch signaling maintains neural rosette polarity. PLoS One. 2013; 8:e62959. [PubMed: 23675446]
36. Kozlovskaja-Gumbrienė A, Yi R, Alexander R, et al. Proliferation-independent regulation of organ size by Fgf/Notch signaling. Elife. 2017; 6:e21049. [PubMed: 28085667]
37. Kovall RA, Blacklow SC. Mechanistic insights into notch receptor signaling from structural and biochemical studies. Curr Top Dev Biol. 2010; 92:31–71. [PubMed: 20816392]
38. Fan B, Malato Y, Calvisi DF, et al. Cholangiocarcinomas can originate from hepatocytes in mice. J Clin Invest. 2012; 122:2911–2915. [PubMed: 22797301]
39. Tanimizu N, Nishikawa Y, Ichinohe N, et al. Sry HMG box protein 9-positive (Sox9+) epithelial cell adhesion molecule-negative (EpCAM-) biphenotypic cells derived from hepatocytes are involved in mouse liver regeneration. J Biol Chem. 2014; 289:7589–7598. [PubMed: 24482234]

40. Walter TJ, Vanderpool C, Cast AE, et al. Intrahepatic bile duct regeneration in mice does not require Hnf6 or notch signaling through Rbpj. Am J Pathol. 2014; 184:1479–1488. [PubMed: 24631193]
41. Nowell CS, Radtke F. Notch as a tumour suppressor. Nat Rev Cancer. 2017; 17:145–159. [PubMed: 28154375]
42. Andersson ER, Lendahl U. Therapeutic modulation of Notch signalling–are we there yet? Nat Rev Drug Discov. 2014; 13:357–378. [PubMed: 24781550]
43. Alvaro D, Metalli VD, Alpini G, et al. The intrahepatic biliary epithelium is a target of the growth hormone/insulin-like growth factor 1 axis. J Hepatol. 2005; 43:875–883. [PubMed: 16083987]
44. Geisler F, Nagl F, Mazur PK, et al. Liver-specific inactivation of Notch2, but not Notch1, compromises intrahepatic bile duct development in mice. Hepatology. 2008; 48:607–616. [PubMed: 18666240]
45. Jeliazkova P, Jörs S, Lee M, et al. Canonical Notch2 signaling determines biliary cell fates of embryonic hepatoblasts and adult hepatocytes independent of Hes1. Hepatology. 2013; 57:2469–2479. [PubMed: 23315998]
46. Falix FA, Weeda VB, Labruyere WT, et al. Hepatic Notch2 deficiency leads to bile duct agenesis perinatally and secondary bile duct formation after weaning. Dev Biol. 2014; 396:201–213. [PubMed: 25446530]

Europe PMC Funders Author Manuscripts

Europe PMC Funders Author Manuscripts

Editor's Notes

Background and Context

Alagille syndrome is caused by mutations in *JAGGED1*, but it is unclear how specific mutations impact on Notch signaling and affect development, and how faithfully Jag1 mutant models mimic the human condition.

New Findings

A receptor-selective missense mutation in mouse *Jag1* (H268Q) recapitulates Alagille syndrome phenotypes in mice. RNA seq of mouse liver samples and samples from patients, showed that apical polarity of bile ducts is severely disrupted.

Limitations

The mouse model is based on homozygous mutation of *Jag1*, while human patients are heterozygous for *JAG1* mutations.

Impact

This new mouse model will allow development and testing of new therapies for Alagille syndrome, as well as a new model in which to study how Notch signaling controls development of organs affected by Alagille syndrome.

Europe PMC Funders Author Manuscripts

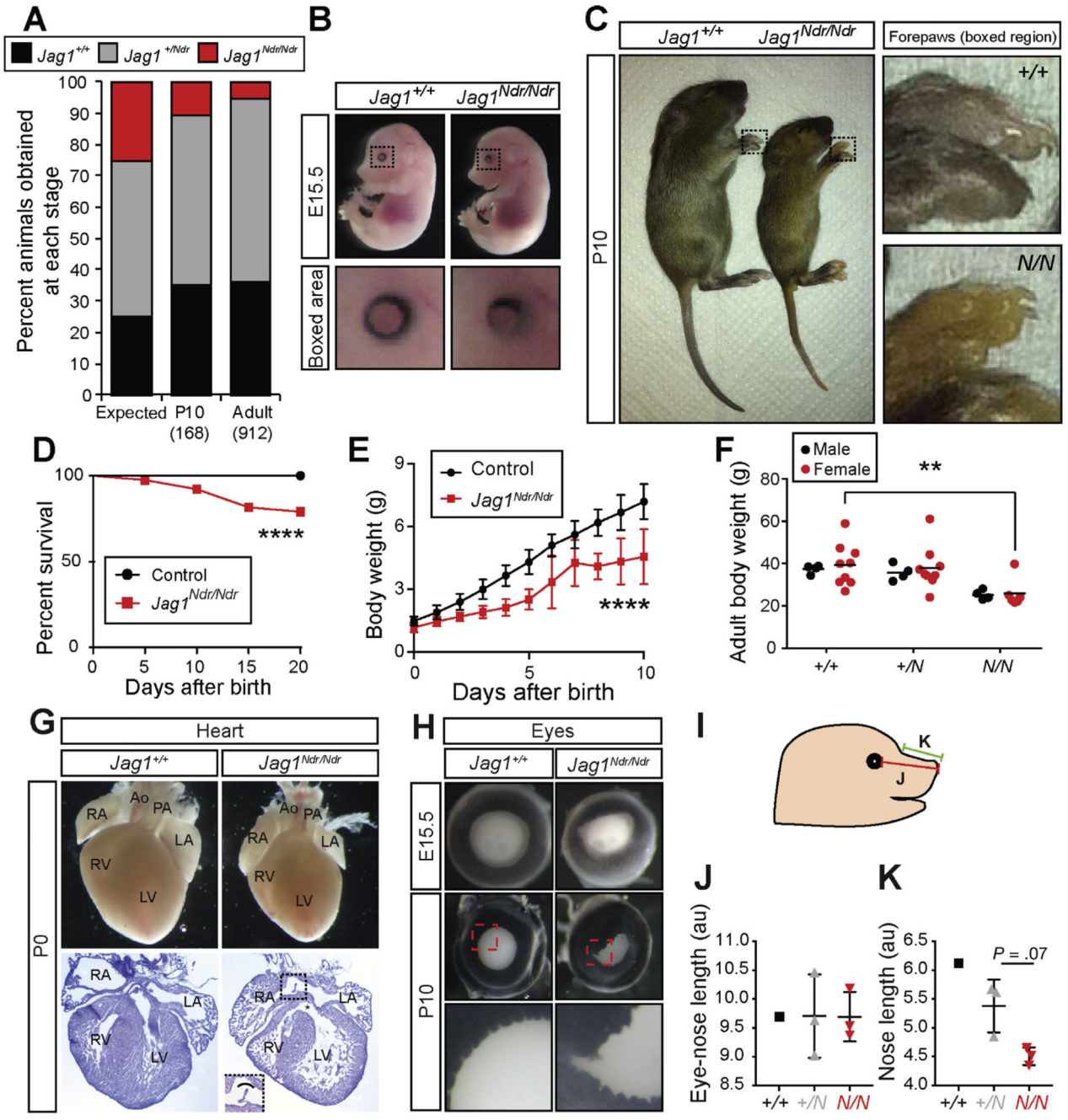

Figure 1.

Jag1$^{Ndr/Ndr}$ C3H/C57bl6 mice survive to adulthood with Alagille-like phenotypes. (*A*) *Jag1*$^{+/Ndr}$ mice were mated to generate *Jag1*$^{+/+}$, *Jag1*$^{+/Ndr}$ and *Jag1*$^{Ndr/Ndr}$ offspring. At P10 and adult stages, fewer than the expected 25% of *Jag1*$^{Ndr/Ndr}$ mice were observed. (*B, C*) At E15.5 *Jag1*$^{Ndr/Ndr}$ mice appear grossly normal, with a mild eye defect (*B*), and by P10 are smaller and jaundiced (*C*). (*D*) After birth, 20% of *Jag1*$^{Ndr/Ndr}$ mice die within the first 20 days. (*E*) At birth, *Jag1*$^{Ndr/Ndr}$ mice are of normal size, but fail to gain weight as rapidly, a difference that is significant from P2, and (*F*) persistently weigh less than wild types. (*G*)

Europe PMC Funders Author Manuscripts

Jag1$^{Ndr/Ndr}$ hearts are somewhat smaller than wild type hearts, likely corresponding to the smaller size of *Jag1*$^{Ndr/Ndr}$ mice. Hematoxylin staining of cryosections reveals ventricular (asterisk) and atrial (boxed) septation defects. (*H*) Iris dysmorphologies are manifested in *Jag1*$^{Ndr/Ndr}$ mice as early as E15.5. (*I*) Craniofacial proportions were measured in photos of E15.5 embryos, measuring the distance from (*J*) the eye to the tip of the snout and (*K*) the snout bridge to the tip of the snout, revealing a tendency towards altered proportions. For *J* and *K*, 3 animals were measured for *Jag1*$^{+/Ndr}$ and *Jag1*$^{Ndr/Ndr}$, but only 1 *Jag1*$^{+/+}$. Error bars indicate s.d.; $^{**}P < .01$, $^{****}P < .0001$.

Europe PMC Funders Author Manuscripts

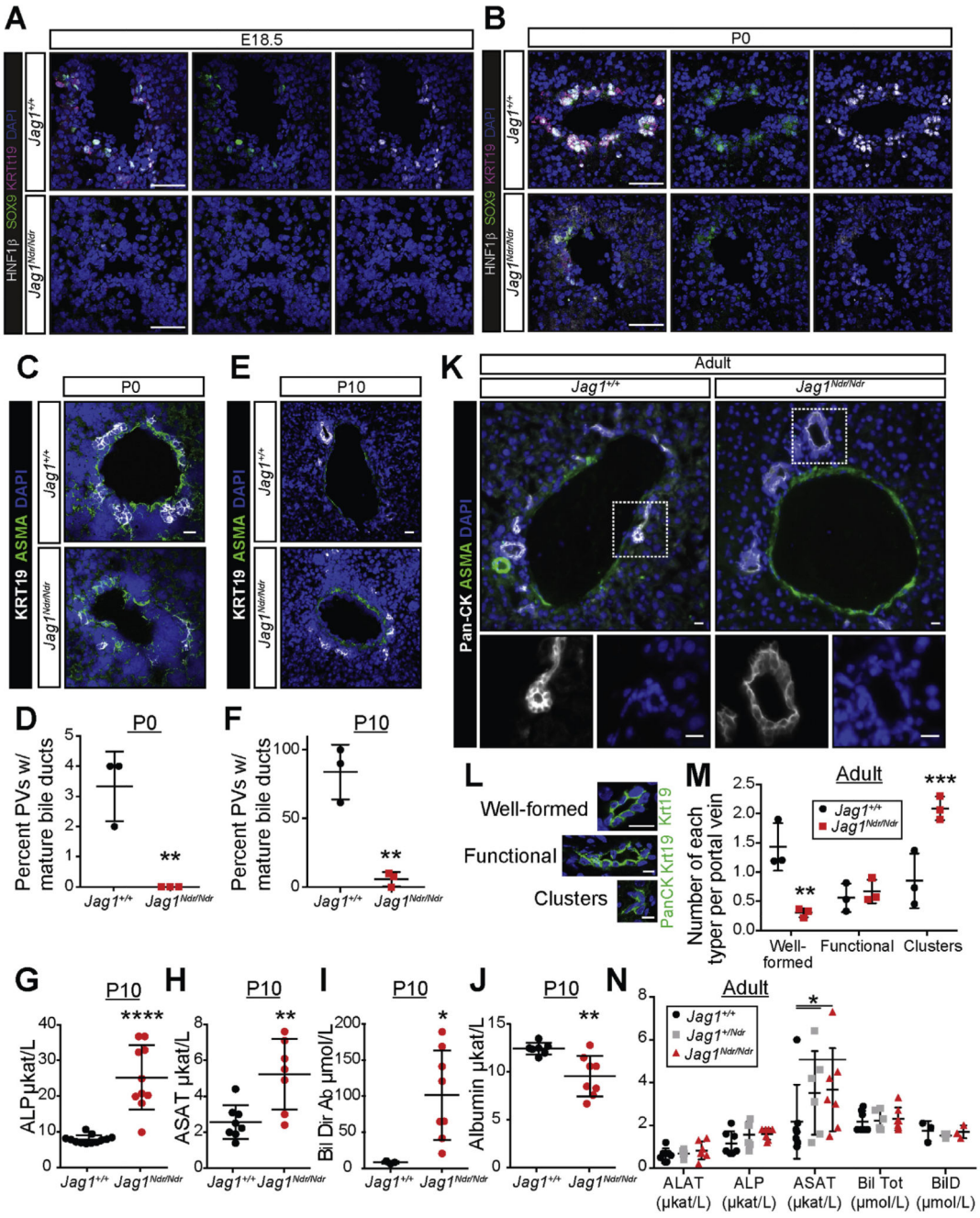

Figure 2.

Postnatal *Jag1*$^{Ndr/Ndr}$ mice display ductopenia, which is rescued in adults. (*A*, *B*) HNF1*β*, SOX9, and KRT19 staining show a marked absence of biliary cells at E18.5 (*A*) and weak staining at P0 (*B*) near the hilum in *Jag1*$^{Ndr/Ndr}$ liver. (*C*, *D*) KRT19^{+} cell clusters appear around ASMA+ periportal regions near the hilum of wild type *Jag1*$^{+/+}$ mice at P0, but are absent in *Jag1*$^{Ndr/Ndr}$ mice. (*E*, *F*) By P10, clusters of biliary cells have lumenized to form ducts in *Jag1*$^{+/+}$ mice, but not in *Jag1*$^{Ndr/Ndr}$ mice. *Jag1*$^{Ndr/Ndr}$ mice display increased (*G*) alkaline phosphatase (ALP), (*H*) aspartate aminotransferase (ASAT), (*I*) direct bilirubin (Bil

Dir), and (*J*) decreased albumin. (*K*) At adult stages, lumenized bile ducts are present in both *Jag1*$^{+/+}$ and *Jag1*$^{Ndr/Ndr}$ mice, though classification (*L*) of structures shows (*M*) significantly more clusters in *Jag1*$^{Ndr/Ndr}$ mice and fewer well-formed bile ducts. (*N*) Nevertheless, markers of liver function demonstrate a rescue of bile duct function in adult *Jag1*$^{Ndr/Ndr}$ mice in most serum chemistry markers. A small difference in aspartate aminotransferase levels persists. Error bars indicate s.d.; **P* <.05, ***P* <.01, ****P* <.001, *****P* <.0001. Scale bars: (*A*, *B*) 50 μm, (*C*) 20 μm, (*I*, *J*) 10 μm.

Europe PMC Funders Author Manuscripts

Europe PMC Funders Author Manuscripts

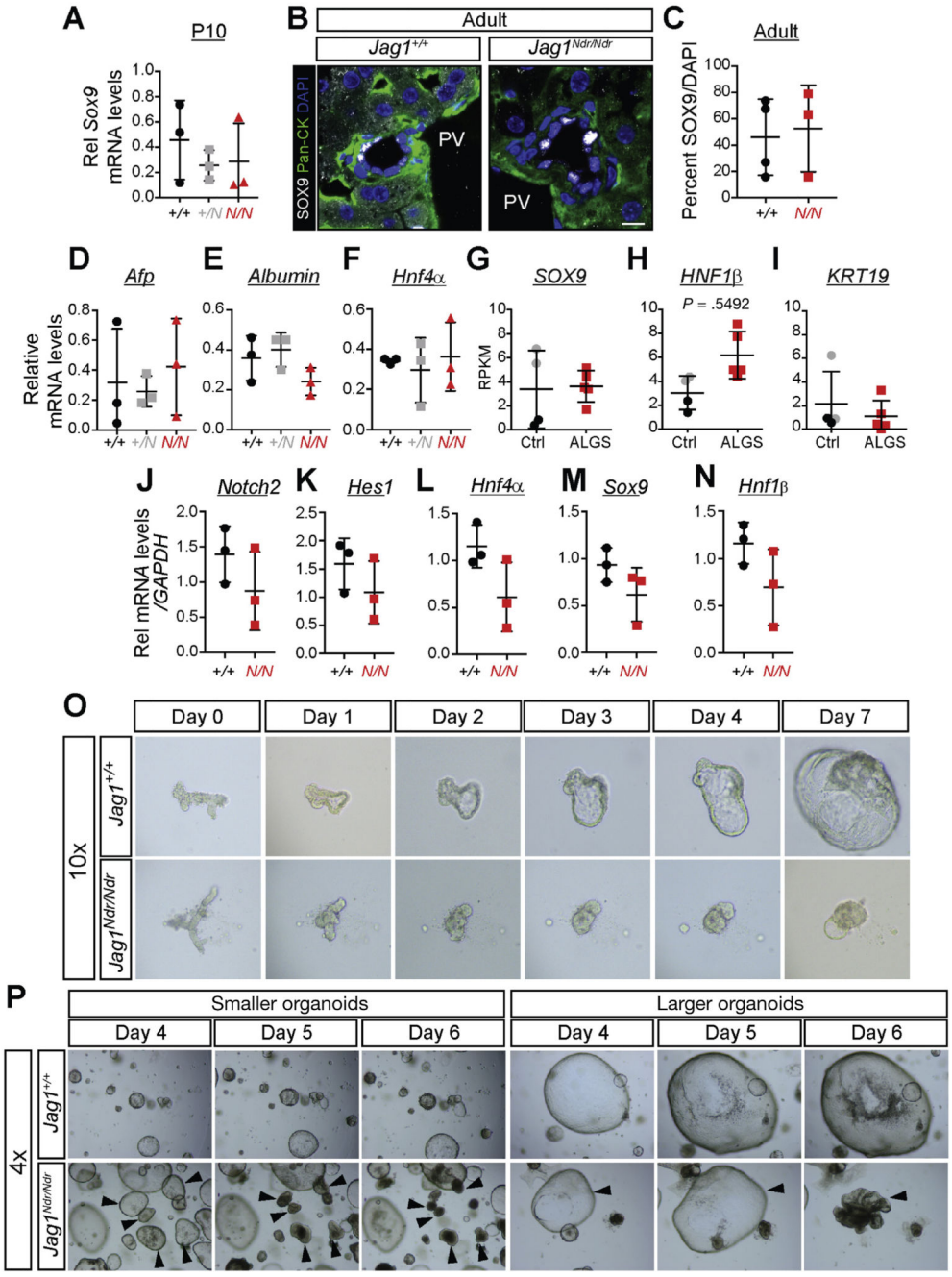

Figure 3.

Jag1$^{Ndr/Ndr}$ biliary cells express the expected markers but display structural instability. Sox9 levels are unchanged at P10 at the mRNA level (*A*), and at adult stages at protein levels (*B*, *C*). qPCR for (*D*) *alpha-fetoprotein*, (*E*) *albumin*, and (*F*) *Hnf4α* show no significant differences in *Jag1*$^{Ndr/Ndr}$ mice at P10. Similarly, RNA sequencing of ALGS livers shows no difference in (*G*) *SOX9*, (*H*) *HNF1β*, or (*I*) *KRT19* levels. Organoids derived from adult *Jag1*$^{Ndr/Ndr}$ livers expressed normal levels of (*J*) *Notch2*, (*K*) *Hes1*, (*L*) *Hnf4α*, (*M*) *Sox9,* and (*N*) *Hnf1β* as assessed by qPCR, but (*O*) grew slowly and (*P*) sometimes spontaneously

collapsed. Collapse was not related to organoid size because both smaller and larger organoids collapsed. No differences were significant. Scale bar: (*B*) 10 μm.

Europe PMC Funders Author Manuscripts

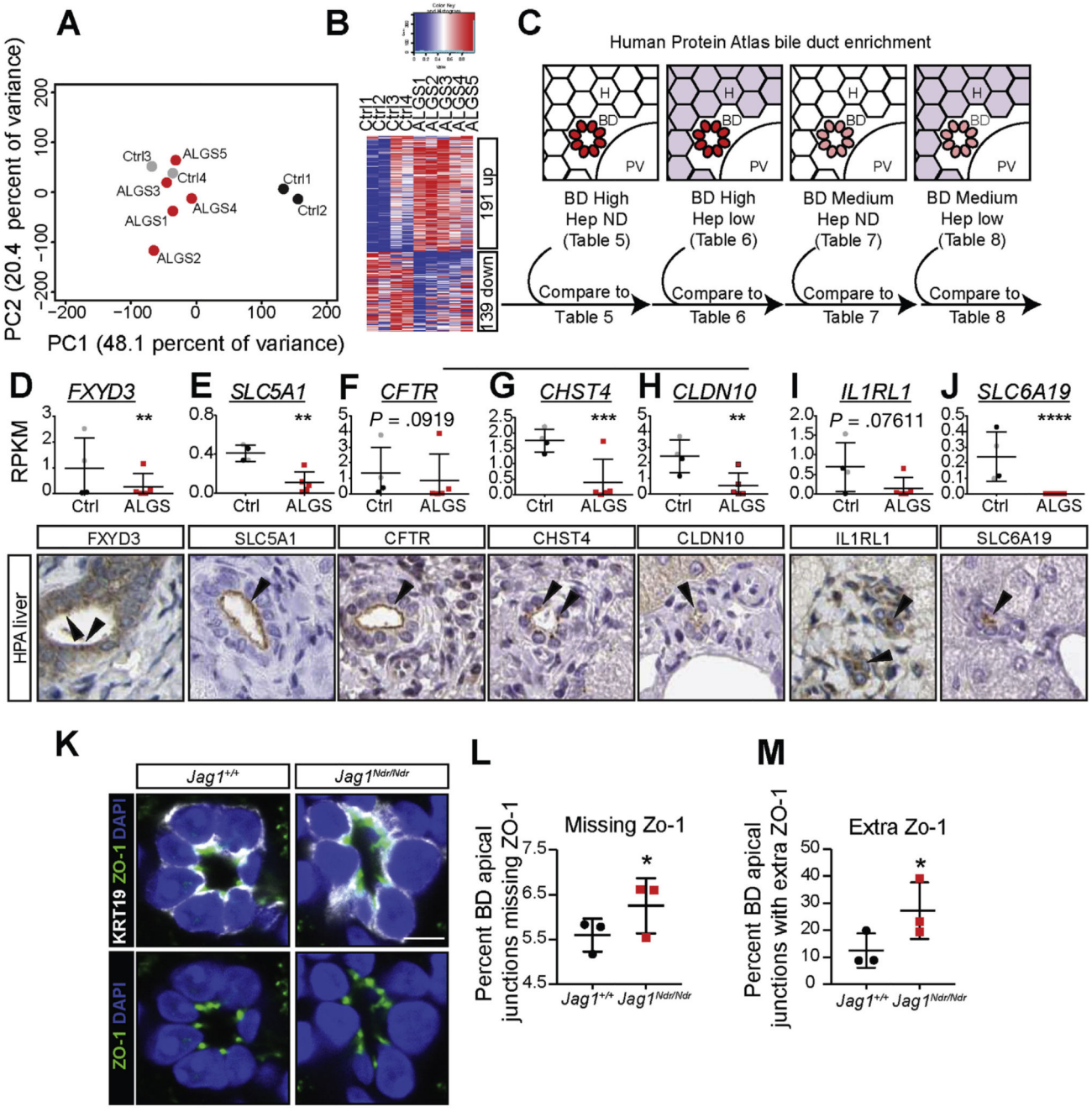

Figure 4.

RNA sequencing of ALGS liver reveals a specific decrease in apical markers of biliary cells. (*A*) Principle component analysis (PCA) of RNA sequencing of liver biopsies from patients with ALGS or control patients. A comparison with non-cholestatic control samples (Ctrl 1 and 2) and with cholestatic control samples (Ctrl 3 and 4) shows that ALGS samples cluster with cholestatic liver samples. (*B*) Heatmap shows 191 significantly up-regulated and 139 down-regulated genes in ALGS samples. (*C*) Dysregulated genes were compared with protein lists generated using the HPA (www.proteinatlas.org)[18] for genes with high/medium

Europe PMC Funders Author Manuscripts

protein expression in biliary cells, and undetected/low expression in hepatocytes (Supplementary Tables 5–8). This pipeline identified transcripts whose proteins were highly enriched at the apical side of bile ducts, including (*D*) FXYD3, and (*E*) SLC5A1. Manual comparison of the top 30 down-regulated genes in ALGS further revealed apically enriched proteins: (*F*) CFTR, (*G*) CHST4, (*H*) CLDN10, (*I*) IL1RL1, and (*J*) SLC6A19. (*K*) *TJP1*/ZO-1 is not down-regulated but is aberrantly localized, with some junctions (*L*) missing ZO-1, and other cell junctions with (*M*) extra ZO1 punctae. Error bars indicate s.d.; **corrected *P*-value (False Discovery Rate) <.01, ***False Discovery Rate <.001, ****False Discovery Rate <10 -7. Scale bar: 5 μm.

Europe PMC Funders Author Manuscripts

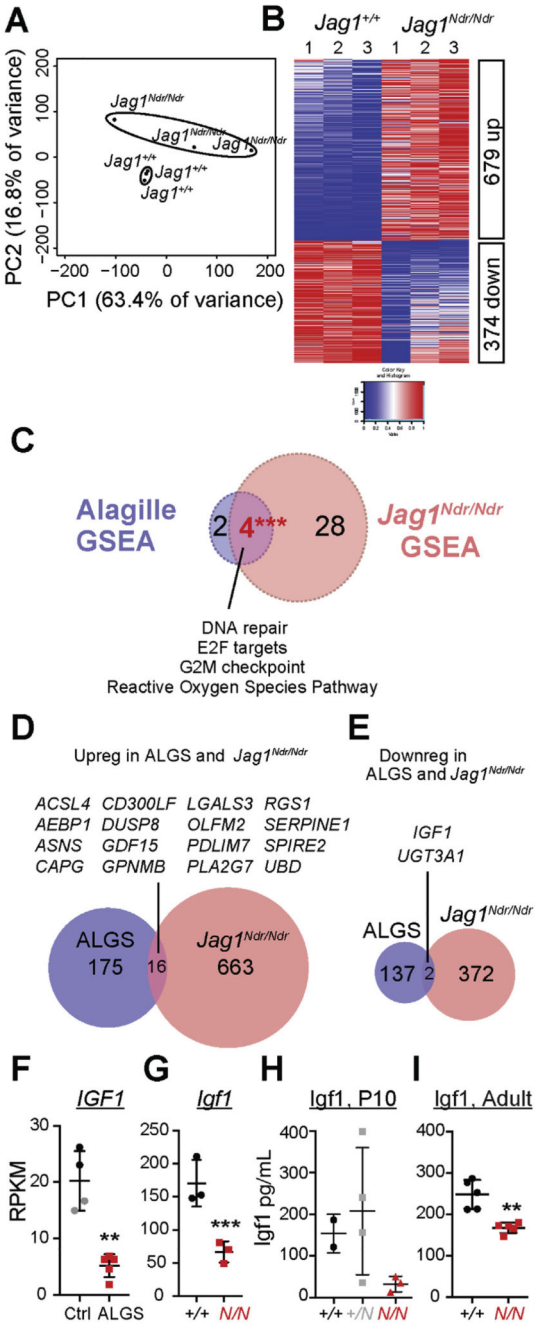

Figure 5.

IGF1 is dysregulated in *Jag1*$^{Ndr/Ndr}$ and Alagille liver. (*A*) PCA of RNA sequencing reveals that *Jag1*$^{+/+}$ and *Jag1*$^{Ndr/Ndr}$ liver transcriptomes cluster distinctly. (*B*) Heatmap shows 679 significantly up-regulated and 374 down-regulated genes in *Jag1*$^{Ndr/Ndr}$ livers. (*C*) Comparison of Gene Set Enrichment Analyses (GSEA), of livers from *Jag1*$^{Ndr/Ndr}$ mice and patients with ALGS (Supplementary Tables 12–15) shows extensive overlap. (*D*) Comparison of significantly dysregulated genes shows (*D*) 16 genes up-regulated and (*E*) 2 genes down-regulated in both *Jag1*$^{Ndr/Ndr}$ mice and ALGS, including *Igf1*. *Igf1* mRNA

levels are highly down-regulated in Alagille livers (*F*) and *Jag1*$^{Ndr/Ndr}$ livers (*G*). IGF1 protein levels were confirmed to be down-regulated in serum of (*H*) P10 and (*I*) adult mice. Error bars indicate s.d.; ***P* <.01, ****P* <.001. (In *F*, and *G*, *P*-values are corrected *P*-values).

Europe PMC Funders Author Manuscripts

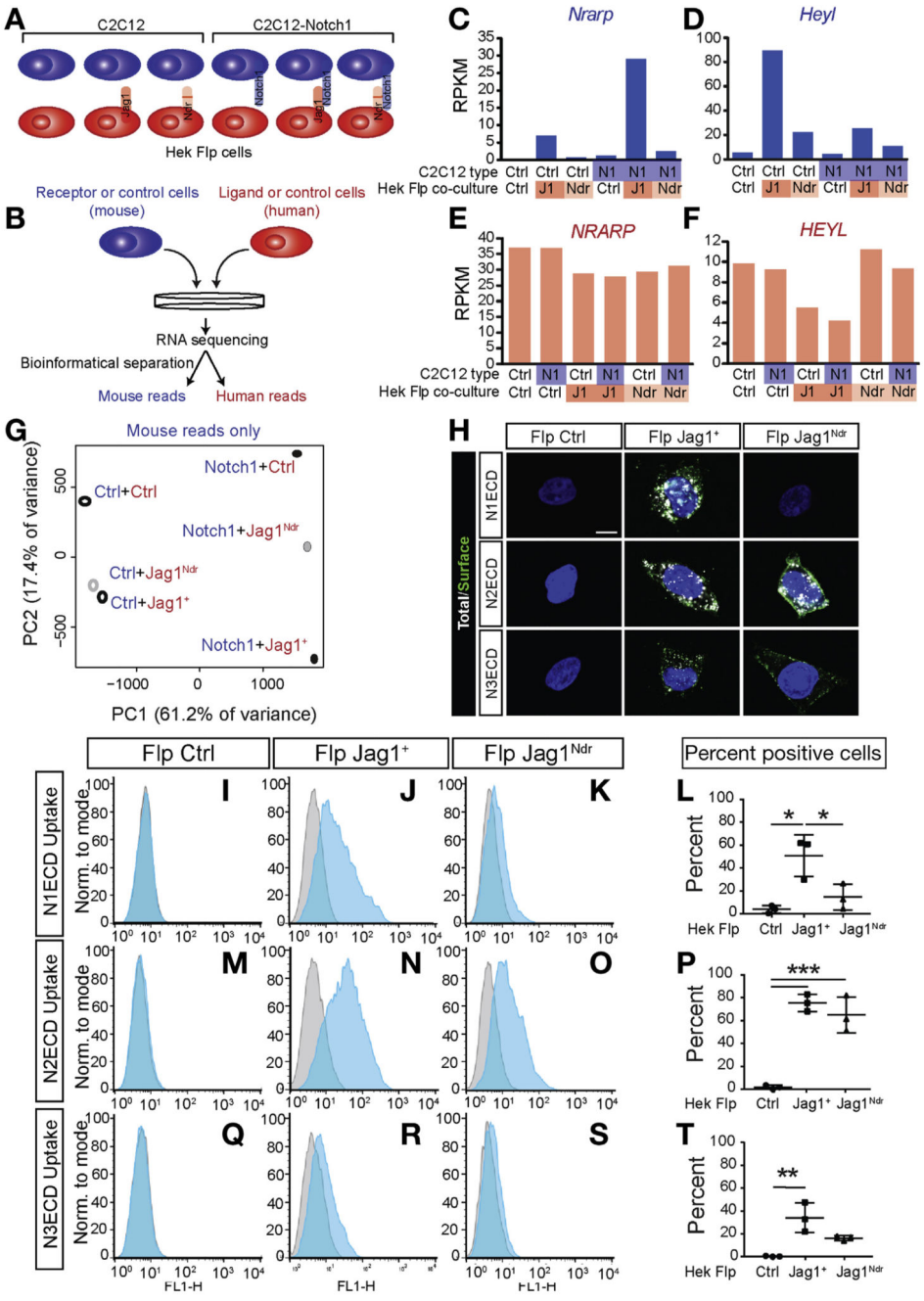

Figure 6.

JAG1^{Ndr} is a Notch signaling hypomorph with receptor-selective binding. (*A*) Scheme depicting co-culture combinations. Control or NOTCH1-overexpressing C2C12 cells (mouse cells, blue) were co-cultured with Flp Ctrl, Flp JAG1^{+}, or Flp JAG1^{Ndr} cells (human cells, red). (*B*) After 6 hours, RNA was extracted for species-specific RNA sequencing (S^3). Bioinformatic analyses separates mouse from human reads. The Notch target genes, *Nrarp* and *Heyl*, are (*C*, *D*) up-regulated in mouse receptor cells upon simulation with Flp JAG1^{+} cells, (*E*, *F*) but not in human ligand cells. (*G*) PCA for the mouse transcriptome shows that

control and NOTCH1-overexpressing C2C12 cell lines both respond to JAG1^{+} stimulation with a similar downwards shift, reflecting Notch activation. JAG1^{Ndr} is only capable of inducing part of this response in Notch1-overexpressing C2C12 cells, but behaves similar to JAG1^{+} in its activation of C2C12 cells. (*H–T*) JAG1^{Ndr} does not bind NOTCH1 but does bind NOTCH2 and NOTCH3. Flp Ctrl, Flp JAG1^{+}, or Flp JAG1^{Ndr} cells were treated with fluorescently tagged extracellular domain of NOTCH1, 2, or 3 (N1-3ECD, white). After 1 hour of uptake, cells were fixed and anti-Fc was used to detect non-endocytosed, cell surface N1-3ECD (green), or cells were subjected to FACS analysis. (*H*) Flp Ctrl cells do not bind N1-3ECD. Flp JAG1^{+} cells bind and internalize NOTCH1, 2, and 3. Flp JAG1^{Ndr} cells do not bind NOTCH1, but do bind NOTCH2 and NOTCH3. FACS analysis of N1ECD uptake by (*I*) Flp Ctrl cells, (*J*) Flp JAG1^{+}, or (*K*) Flp JAG1^{Ndr} cells, quantified in (*L*). FACS analysis of N2ECD uptake by (*M*) Flp Ctrl cells, (*N*) Flp JAG1^{+}, or (*O*) Flp JAG1^{Ndr} cells, quantified in (*P*). FACS analysis of N3ECD uptake by (*Q*) Flp Ctrl cells, (*R*) Flp JAG1+, or (*S*) Flp JAG1^{Ndr} cells, quantified in (*T*). Quantifications (*L*, *P*, *T*) show Overton cumulative histogram subtractions. Error bars indicate s.d.; **P* <.05, ***P* <.01, ****P* <.001. *C–G* represent results from 1 experiment. Scale bar: (*H*) 10 μm.

Europe PMC Funders Author Manuscripts

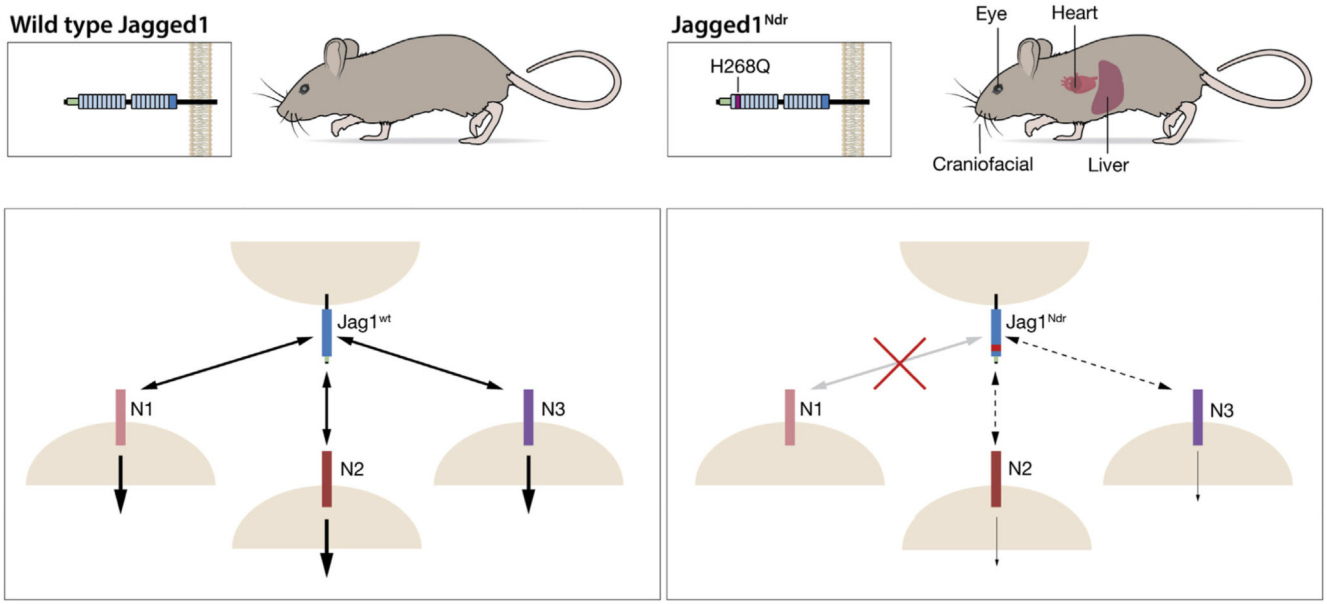

Figure 7.

Schematic summary of phenotypes and signaling aberrations in *Jag1*$^{Ndr/Ndr}$ mice. The location of the JAG1^{Ndr} mutation, organs with phenotypes described here, and the interaction and signaling dysregulation for individual Notch receptors are depicted.

Europe PMC Funders Author Manuscripts